2mit

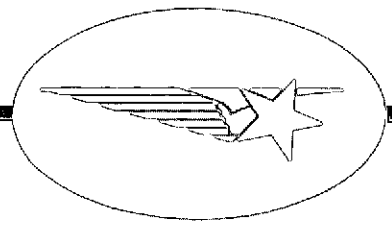

Lockheed

MISSILES & SPACE COMPANY

A GROUP DIVISION OF LOCKHEED AIRCRAFT CORPORATION

SUNNYVALE, CALIFORNIA

LMSC/D387326
GCS/3529/6211
74 Mar 12

QUARTERLY PROGRESS REPORT NO. 2

ANALYSIS OF DATA FROM SPACECRAFT (STRATOSPHERIC WARMINGS)

NASA CONTRACT NASW-2553

NASA HEADQUARTERS, WASH. D.C.

COVERING THE PERIOD DECEMBER 1973 - FEBRUARY 1974

CONTRACT MONITOR: H. D. CALAHAN
NASA HEADQUARTERS (CODE SG)
WASHINGTON, D.C. 20546

PROJECT LEADER: R. WEISS
LOCKHEED MISSILES & SPACE CO., INC.
SUNNYVALE, CALIF. 94088

PRINCIPAL CONTRIBUTOR: A. D. ANDERSON
ATMOSPHERIC PHYSICS BRANCH
RADIATION PHYSICS LABORATORY

TABLE OF CONTENTS

1. INTRODUCTION

The primary objectives of the study are to establish the details of the stratospheric warming processes as to time, area, and intensity and to correlate the warmings with other terrestrial and solar phenomena occurring at satellite platform altitudes or observable from satellite platforms. Early correlations will be statistical and are expected to point to the mechanisms that are connected or are unconnected. The main purpose of the study is to find if there are links between the perturbed upper atmosphere (mesosphere and thermosphere) and the stratosphere that could explain stratospheric warmings.

Stratospheric warmings are large-area phenomena containing great amounts of energy. They probably have major influence on the weather over large areas, on observations from satellites and high-altitude platforms, on the dynamics of the upper and lower atmospheres, on atmospheric chemistry, on air pollution observations and on backgrounds for surveillance and earth resources observations.

Little correlative data has been brought to bear on defining the relationship between energetic events above 50 km and the warmings at about 40 km. Current rocket and balloon-borne IR sounding instruments do not provide good coverage on a global basis. It is difficult to provide dynamic readings throughout a warming by means of ground based instrumentation. Satellite and other high altitude data, therefore, need to be applied to the problem.

Although meteorological analyses indicate that the warmings result from the transfer of energy from the troposphere to the stratosphere, the initiating or trigger mechanism is unknown. In other words, no one has attempted to predict stratospheric warmings. The emphasis of this effort is to attempt to find clues to possible trigger mechanisms arising in the upper atmosphere or solar activity. Several steps are involved: (a) Determine from the literature possible correlations of warmings with geophysical events; (b) Find solar and geophysical indices that represent the pertinent events; (c) Define the stratospheric warming events (start, maximum, end) so that these indices may be applied to uncover the trigger mechanism(s). Existing data and literature have been searched to find the identified cases of stratospheric warmings. Six case histories of these events have been chosen by assembling correlative high altitude satellite, rocket and ground based measurements, geophysical characteristics and solar activity data. Existing data from NIMBUS spacecraft sensors such as the MRIR, SIRS, IRIS, and SCR are being used to define the existence and characteristics of the warming in the 20-50 km-altitude regime. Data from various particle and radiation experiments on ALOUETTE, ISIS, OGO, and OSO satellites are being used to determine some of the energetic conditions existing in the upper atmosphere prior to and during the warming events. The correlation of the particle data with the lower altitude radiance data may lend some insight into the physical mechanism of sudden warmings. Then statistical analyses will be carried out with various influencing factors and effects to see if a cause and effect relationship is discernible. Finally, comparison of results will be made with existing spatial and temporal models of warming events. It is hoped that the models may be extended as a result of this study.

2. SUMMARY OF ACTIVITIES

The main effort of this period concentrated on the further definition of the problem of defining links between the upper atmosphere and the stratosphere, and the role of geophysical and solar indices. The collection of relevant data was continued, and the analysis of specific cases started.

An updating was performed of the literature search presented in Quarterly Progress Report No. 1 (Appendix E). One additional case was identified for further study and support data for that case was collected. Further study of the literature resulted in the further definition of the problem of identifying links between the upper atmosphere and the stratosphere. Expanded definition includes discussions of the nature and potential sources of stratospheric warmings (Appendix A), the potential mechanisms for their correlation with geophysical events (Appendix B), and the significance and sources of various potentially correlated solar and geophysical indices (Appendix C).

The analysis of the two stratospheric warmings (Cases 4 and 5) occurring in the 1969-1970 and 1970-71 winters has been completed during the quarter.

3. TECHNICAL ACTIVITIES

3.1 Task A - Development of Case Histories. Work during this report period concentrated on the development of warming histories for the identified sudden warmings cases. The characterization of a warming event is not a simple matter because of its four dimensionality and because adequate temperature field data are not available. The events may be defined for analytic purposes by a beginning, maximum, and end relating to each altitude that it affects.

The highest altitude for which routine temperature data are available on a daily basis in the form of charts is the 10 millibar pressure altitude, corresponding to approximately 31 kilometers. These charts, available from the National Weather Service in microfilm form, cover only the Northern Hemisphere. Because of their immediate availability, these charts, together with the constant pressure charts at lower pressure altitudes (30 and 50 mb) were used to define the existence and areal extent of the identified Northern Hemispheric warming events. The fact, however, that the warmings typically occur at higher altitudes (see Appendix A, for example), and that they are not confined to one geographic area, makes it mandatory to seek other sources of data for a fuller description of the warming. These additional data are derived from rocketsondes, analysis of meteor winds, and remote "soundings" from satellite-borne instruments (e.g., SIRS, SCR, ITPR, VTPR on Nimbus and NOAA-2). These data have been utilized wherever possible to derive a four-dimensional description of each warming event. Specifically, the analytic technique of deriving 1 mb temperatures using the upper channels of the SCR has provided information on a warming occurring in mid-February 1972 at 45 km which was largely unnoticed by users of in-situ data only since it occurred at altitudes higher than normal balloon sonde altitudes. This case has been added to the list of cases to be analyzed if time permits.

Upper atmosphere researchers interested in the stratospheric warming phenomenon have gathered a large amount of supplementary data describing these events. A trip was made during this report period to obtain some of these data to expand the description of the selected cases. The visit to Roderick S. Quiroz, Upper Air Branch, National Meteorological Center, Washington, D. C., yielded a large number of Northern Hemisphere charts at and around times of known warmings. The charts were derived from Satellite radiance measurements by the Nimbus-IV SIRS and SCR covering the 1970-71 warming (Case 5), Nimbus-III SIRS covering the 1969-70 warming (Case 4), and NOAA-2 VTPR charts covering the 1973 warming (Case 6).

A second visit was made to Dr. Sigmund Fritz, National Environmental Satellite Service, Suitland, Maryland, to obtain digital maps of radiance for the upper channel of the Nimbus III SIRS for the periods including the three identified Southern Hemisphere warmings (Cases 1-3). Radiance from this channel (Channel 8, 668.7 cm^{-1}) represents energy received from a ± 15 km wide band centered at 31 km.

3.2 Task B - Examination of Correlations

There are many possible correlations between geophysical events at high and low altitudes. Many of these were investigated with the aim of selecting those that could trigger stratospheric warmings. Based on this survey (Appendix B) 11 solar and geophysical indices were selected for analysis. Two indices were added to the list previously presented. These 11 indices (listed in Table 1, Appendix C) were generally available on at least a daily basis for most warmings. These indices are described in detail in Appendix C. It is not claimed that this list is complete, but on the basis of the investigation done to date, the indices listed show the greatest promise of describing measureable effects which may yield links to stratospheric warmings.

Appendix B is a discussion of the physical mechanisms for warmings and an introduction to those measurable physical mechanisms which may enter into the stratospheric warming process or act as a trigger. Appendix C amplifies on the solar and geophysical indices which were selected as being potentially related, and discusses each index in detail, giving source and meaning of the measurement. A chart is given which summarizes the available information used in this study.

The analysis of two stratospheric warming cases has been completed (Cases 4 and 5, 1969-70 and 1970-71 winter warmings). Each analysis consists of two parts, i.e., a detailed discussion of the warming as measured by in situ and satellite infrared instrumentation, and a discussion of the potential geophysical correlations. The method is much the same as was indicated in Fig. C-9 of the Quarterly Progress Report No. 1. Results so far are tentative and will be reported in the final report.

3.3 Task C - Extension of Existing Models. No positive correlations have been found to date, and the extension of existing models to higher altitudes would depend on the postulation of a specific mechanism for energy transfer during a warming. Requests have been made for satellite analytic soundings in an area around two known warmings. Dr. E. J. Williamson of Clarendon Laboratory, University of Oxford, the SCR principal investigator, notified us as to his "reluctance to provide anything (referring to individual SCR soundings) but a very few individual samples." The SCR soundings would have been useful in extending our descriptions of warmings to 1 mb pressure altitudes. A request for SIRS soundings for Case 5 is still pending at the Environmental Data Service. These soundings, however, only extend to 10 mb and will be of questionable value if received.

4. PROGRAM STATUS

As of the end of the second quarter of the study, 79 percent of the contracted effort has been completed with 78 percent of the contract resources expended. The data collection supporting development of stratospheric warming case histories has essentially been completed. Two cases have been analyzed, and the remainder are in process. Sections of the final report have been completed and have been included as appendices to the two Quarterly Reports. The first draft of the final report is scheduled to be available at the end of March (Figure 1). The current forecast is for a 1-1/2 man level effort for the month of March (Fig. 2) to complete the analyses of correlations for the selected cases and to complete the final report draft. Contract resources are expected to be adequate assuming that no large rewrite is required.

MASTER CONTRACT SCHEDULE

TECHNOLOGY SUPPLEMENT

NASW-2553 (HEADQUARTERS)
CONTRACT/PGM Nº

PAGE Nº 9 OF ____

TITLE: ANALYSIS OF DATA FROM SPACECRAFT-STRATOSPHERIC WARMINGS

CONTRACT TYPE CPFF

STATUS DATE 3-3-74

VALUE (LESS FEE) $ 30K

START 8-27-73 COMPL 5-26-73

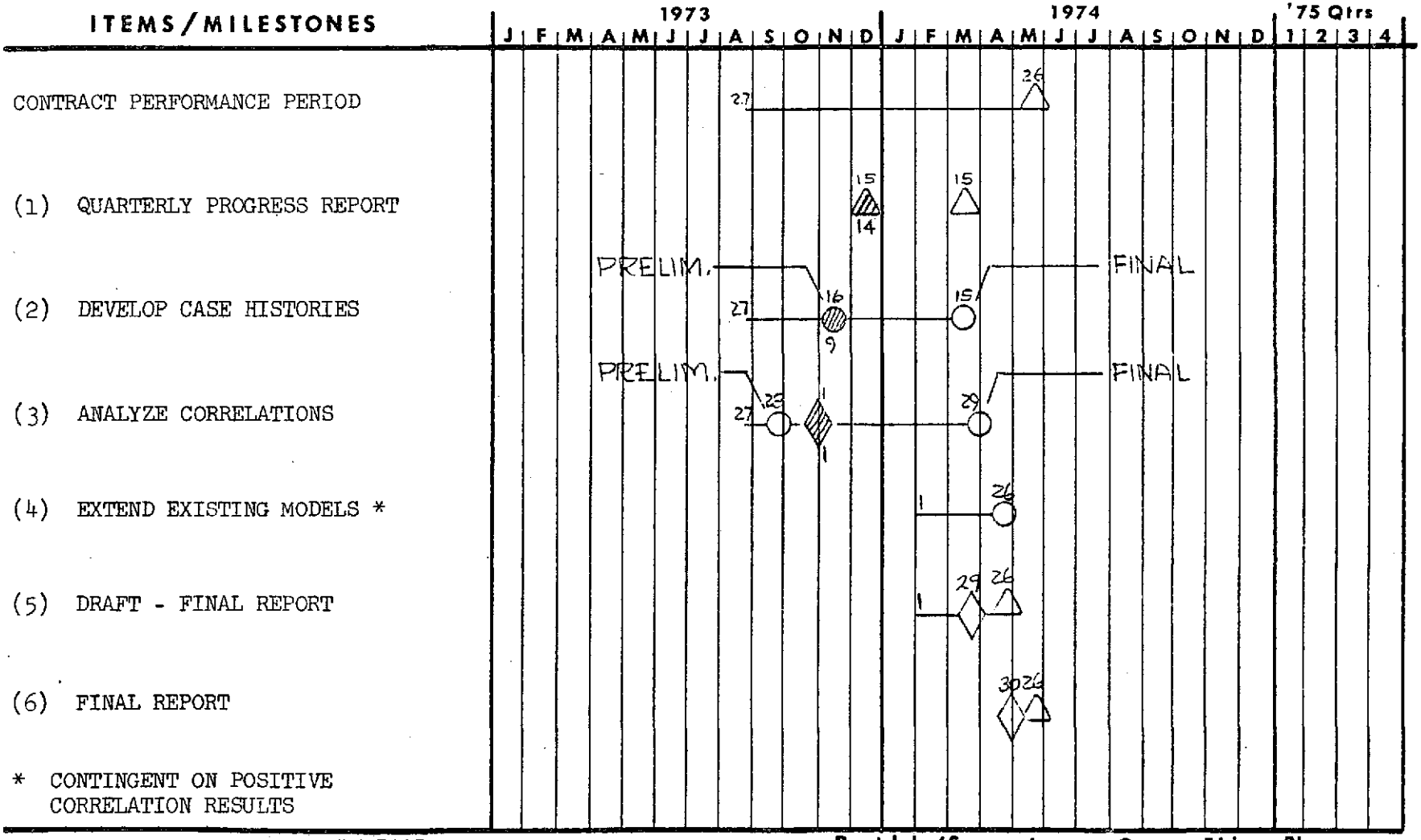

LEGEND
(shown by Schedule/Actual)
△/▨ CONTRACT ◇/▨ ECD ○/▨ INTERNAL MILESTONE
– – – – EXTENDED EFFORT

Proj.Ldr/Support	Orgn	Bldg	Phone
R. WEISS	62-11	104	3-1664
J. R. BUCKLEY	25-39	104	3-0405
T. J. CONRY	67-21	104	2-4072
J. A. HILLHOUSE	67-30	104	2-3580

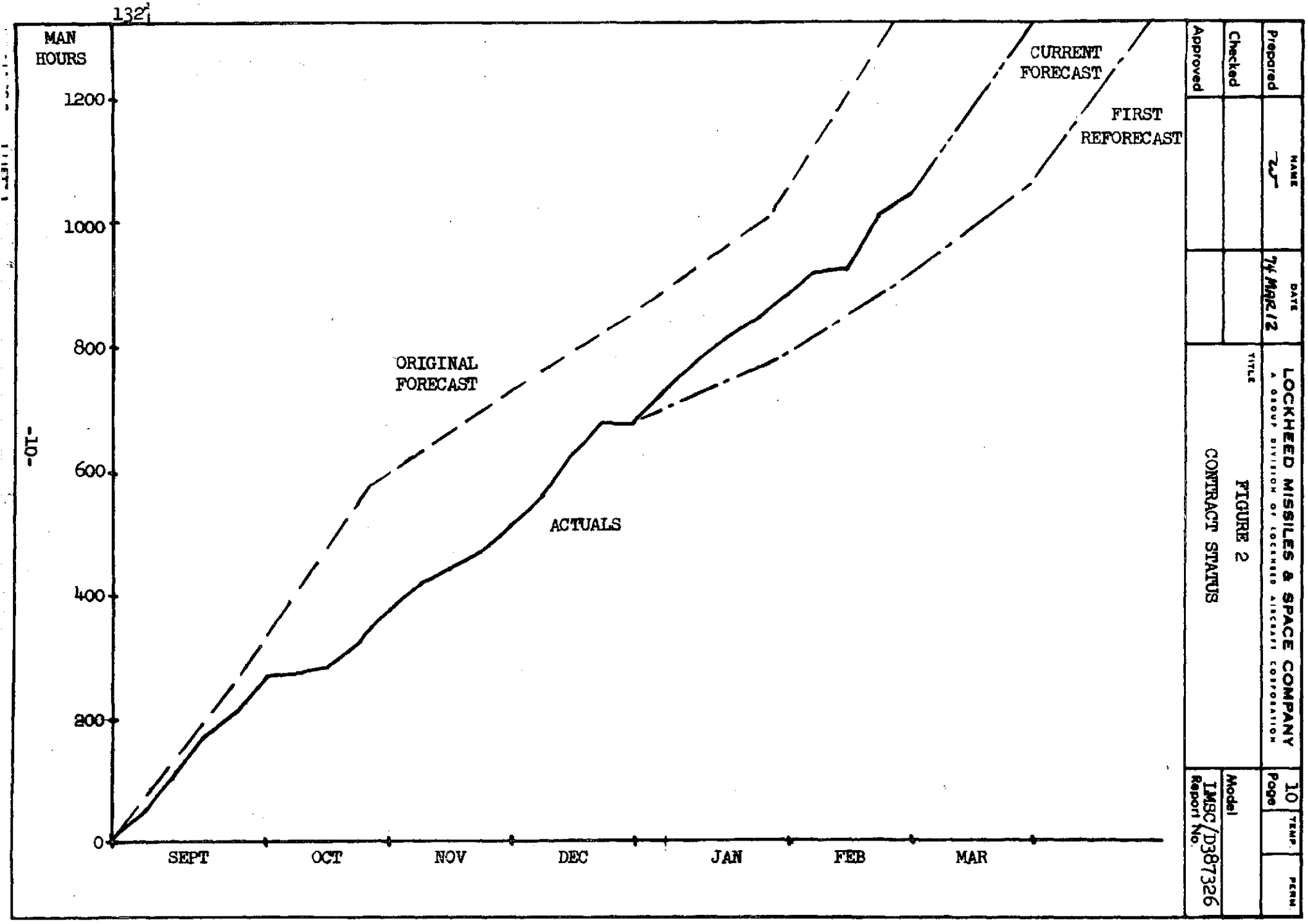

LOCKHEED MISSILES & SPACE COMPANY
A GROUP DIVISION OF LOCKHEED AIRCRAFT CORPORATION

Prepared | Checked | Approved
NAME
DATE 7th MARCH 12

TITLE
FIGURE 2
CONTRACT STATUS

Model
IMSC/D387326 Report No.

Page 10
TEMP
PERM

5. PLANNED ACTIVITIES

The following activities are planned for the final report period.

1. Descriptions of remainder of the warming cases will be completed.

2. Analysis of correlations with geophysical indices will be completed.

3. Conclusions will be recorded as to the presence of measurable links between the upper atmosphere and the stratosphere, and to the potential physical mechanisms involved.

4. A draft of the final report will be provided for review and approval.

APPENDIX A - STRATOSPHERIC WARMINGS

A dynamic event in the stratospheric circulation which is principally characterized by a temperature increase in polar regions immediately above the stratonull level greater than 50°C over a period of ten days or less, accompanied by a disruption of the usual westerly zonal circumpolar flow of the stratospheric winter circulation, is called a Stratospheric Warming.

Stations centered under the warming region as it sweeps poleward provide a very dramatic record of the magnitude of events which must be in progress in the upper atmosphere. Temperature increases of from 30° to 90°C over a period of a week are the rule, and stratospheric wind changes of the order of 100 meters/sec out of the west to 50 meters/sec from the east are common (Webb, 1966).

Figure 1 contains a sequence of rocket soundings from West Geirinish, Germany, taken during a major warming in the winter of 1967-68 (Labitzke, 1971). Profile 1 indicates the beginning phase of the warming with the maximum warming at 60 km (+11C). In Profile 2, the maximum warming has descended to 46 km and increased to +18C. Profile 3 (21 Dec. 1967) the maximum warming is at 43 km and the temperature is +40C. Profile 4 represents a decreasing phase; maximum warming at 44 km has decreased to -4C. Profile 5 is an average atmospheric temperature profile from Groves (1970). Comparison of Profile 5 with the other profiles indicates that the warming affected a depth of atmosphere of approximately 34 km.

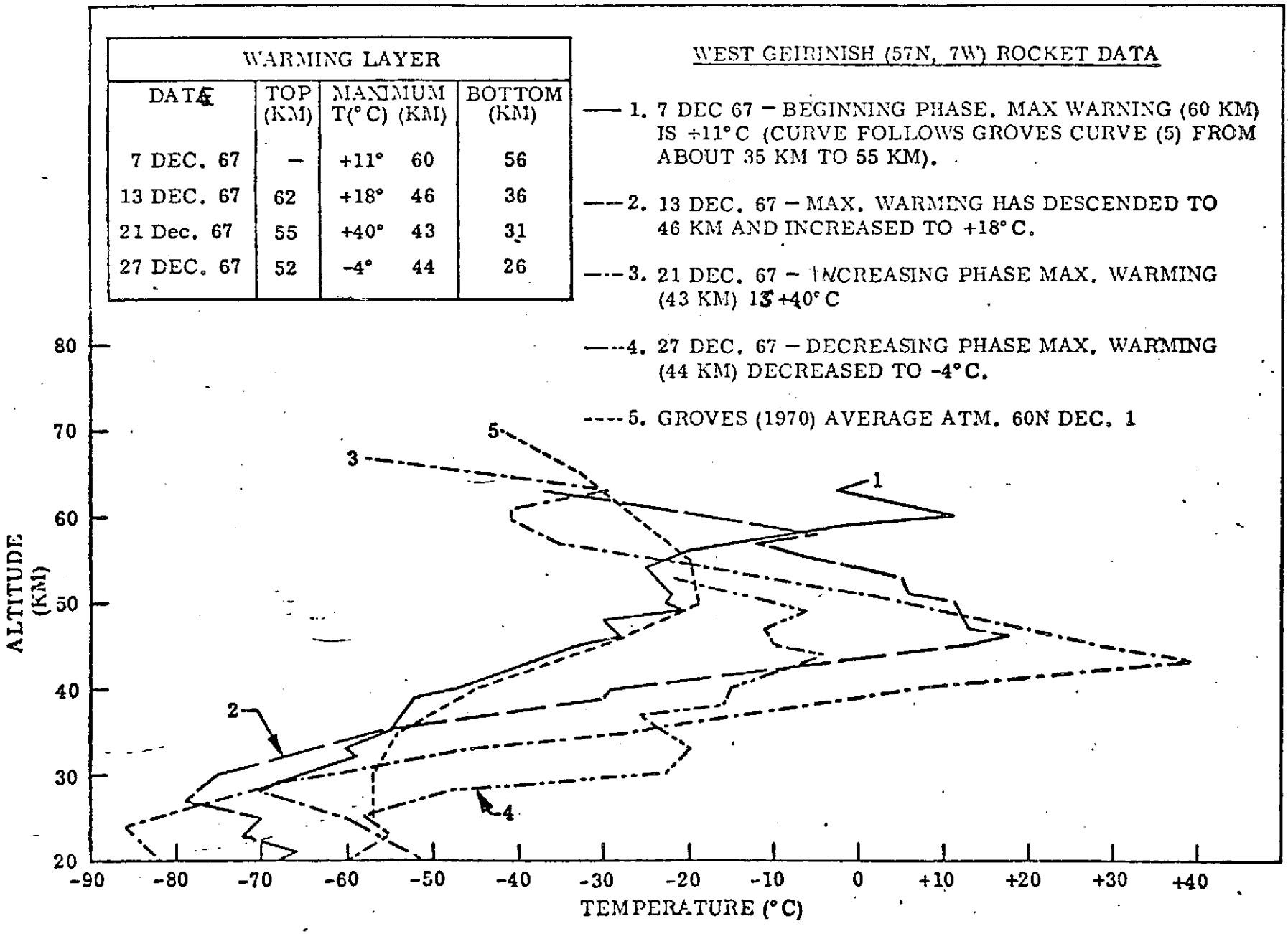

FIGURE 1 WEST GEIRINISH ROCKET DATA DURING WARMING

Stratospheric warmings are large-area phenomena containing large amounts of energy. They probably have major influence on the weather over large areas, on observations from satellites and high-altitude platforms, on the dynamics of the upper and lower atmospheres, on atmospheric chemistry, on air pollution observations and on backgrounds for surveillance and earth resources observations.

Little correlative data has been brought to bear on defining the relationship between energetic events above 50 km and the warmings at about 40 km. Current rocket and balloon-borne IR sounding instruments do not provide good coverage on a global basis. It is difficult to provide dynamic readings throughout a warming by means of ground based instrumentation. Satellite and other high attitude data,therefore, need to be applied to the problem.

Although stratospheric warmings have been studied extensively since their recognition in 1952, their characteristics are not well known or established. They occur mostly in winter and early spring seasons and show largest temperature changes in the northern and southern high-latitude regions. They start at 50 km or above and later sometimes appear at lower levels, penetrating to 25 to 35 km. The energy density of direct solar radiation on an element of atmosphere is smaller by many orders of magnitude than that required to explain the atmospheric temperature rise during a warming. Integration of this energy over time and area would be required to explain a warming in terms of direct heating. The heat input into a

square cm column of the stratosphere between 30 and 50 km altitude needed to raise the temperature 50°K amounts to some 5×10^9 ergs cm^{-2}. Reported warmings may cover 10^{15} cm^2 so the total energy involved can be in excess of 10^{24} ergs. This energy might be compared with 5×10^{23} ergs reported in the solar storm of 11 February 1958 in the red arc aurora, and a computed total solar particle energy of 10^{25} ergs in such a storm. Muench (1965) considered the energy transformations during the stratospheric warming of 22-24 January 1958. His analysis indicated that the energy increase was caused almost entirely by a transfer of energy from the troposphere to the stratosphere. A report by Hirota (1967) on an observed upward propagation of stratospheric warming events supports this conclusion. Matsuno (1971) treated the interaction of vertically propagating planetary waves from the troposphere with the zonal flow in the stratosphere. His model produces many observed features present in stratospheric warmings. Trenberth (1972) used a model of this type to study stratospheric warmings. His model reproduced realistic stratospheric warmings in late winter. Although Trenberth neglected the chemistry, Clark (1970) had previously used a similar model (with somewhat fewer spherical harmonics and coarser vertical resolution) which did include the simple Chapman scheme of oxygen photochemistry. Clark was able to reproduce numerically the observed tendency for the large-scale motion field to shift the maximum of vertically integrated ozone poleward from the low-altitude source region. In such a model, the chemistry interacts with the dynamics via the heating rate Q, which will depend not only on infrared radiation and a parameterization of small-scale convection in the troposphere, but also the absorption of radiation by the variable amount of ozone.

A survey of recorded major and minor stratospheric warmings shows that in January of every year between 1966 and 1971 at least one event occurred in the Northern Hemisphere between 45° and 80° latitude. These same years produced events in the Southern Hemisphere in July and August.

The Problem Of Defining a Given Stratospheric Warming Event

A given stratospheric warming (SW) can be defined provided that the date and time of its start, maximum and end can be determined from the temperature at all altitudes that it affects. One major problem with characterization of SWs occurring in the past is that they occur at altitudes between about 20-65 km (Fig. 1). Until recently, the higher altitudes were only accessible to measurement with meteorological rockets. There are several disadvantages for defining warmings with rocket data. Although there are currently more than 20 meteorological rocket launch sites, these are mainly land-based in the Northern Hemisphere. Hence, the coverage is uneven. Also, the launches are made closer to a weekly than daily basis. However, even if daily launchings were made, this would be insufficient to characterize warmings, inasmuch as the warming centers probably would not lie over the rocket launch sites. In addition, the warming centers move.

The coverage and launch frequency of radiosondes carried by balloons is much better. There are at least 20 times as many radiosonde launch sites than rocket sites. The coverage is best in the Northern Hemisphere over land; the coverage is much poorer in the Southern Hemisphere because of the greater amount of water area. Also, the launch frequency (one to four times daily) is much greater than rockets. The main disadvantage is that only the lower altitudes at which SWs occur are accessible to the balloons (ceiling altitude about 30 km). The 10-mb surface (31 km) is the highest pressure altitude for which hemispheric charts, derived mainly from radiosonde data, are available from the National Weather Service on a daily

basis for the Northern Hemisphere warmings occurring during December 1969 - January 1970, December 1970 - January 1971, and January 1973 - February 1973.

The real hope for the future lies in satellite remote sensing techniques that scan worldwide twice daily. One example is the NIMBUS SIRS instrument data from which temperature profiles can be derived for the altitudes of interest on a worldwide basis. At present, there are some problems in obtaining data at the higher altitudes above 50 km. Therefore, at this time, the analysis of a given SW must be based on radiosonde, rocketsonde, and satellite (radiance) data. The smallest time interval that can be used in characterization is about one day. It is not possible to specify warming start, maximum, or end at a given altitude in a time interval less than about one day. The definition must be incomplete for the warmings considered in this report because little data is available at the higher altitudes above 40-50 km. The radiance measurements made by the SCR on Nimbus 4 provide radiation information from the highest levels in the atmosphere so far obtained. Descriptions of the instrument can be found in the literature (Houghton and Smith, 1970) and the method used by the Oxford University Group to derive temperature profiles from the six radiances using a maximum probability technique has been described by Rodgers (1970). A series of daily charts for levels up to 1 mb (48 km) were constructed to cover the major northern hemisphere warming period in the middle of February 1972.

APPENDIX B

Possible Correlation of Warmings with Geophysical Events

Stratospheric warmings favor the winter and early spring seasons; they exhibit the greatest change of temperature in the polar regions. They start at 50 km or above and later sometimes appear at lower levels. In some cases, the warmings do not penetrate downward as far as 30 km. These very high level relatively limited stratospheric warmings may represent the effects of comparatively limited penetration of the atmosphere by solar corpuscular emanations of only light to moderate intensity, which should be expected to occur not infrequently.

The major warmings of February 1952 and January 1963, which came well after the years of highest sunspot activity, both followed sudden bursts of strong geomagnetic disturbance with a moderate increase of sunspots, and in 1952 with a strong auroral display. The geomagnetically quiet years of 1953-1955 and 1964-1966 were apparently strikingly lacking in stratospheric warmings. The fact that of the sixteen years, 1951 to 1966 inclusive, the only six years lacking stratospheric warmings were also the six geomagnetically most quiet years would seem significant. With the exception of one weak warming at the beginning of March 1956, all 14 warmings, plus the two occurring in February 1952, originated during the months of January and February, when Northern Hemispheric auroral activity is very high, rising to a presumed early March peak frequency which may be even earlier in arctic latitudes. It is to be noted that none of them occurred during December, the month of the presumed winter solstice minimum of auroral frequency, and definitely the coldest month in the arctic stratosphere. During the period 1951-1966, all of the observed sudden

stratospheric warmings developed on the northern geomagnetic pole side of the geographic pole, i.e., essentially in the equatorward dip or trough of the zone of maximum auroral frequency.

The correlation of the time and space distribution of auroral activity with sudden changes of stratospheric temperature indicate that a possible extraterrestrial control, perhaps solar corpuscular invasions of the upper atmosphere which produce auroras and strong geomagnetic disturbances. If solar corpuscular invasions are to cause and control the entire syndrome of associated auroral, and thermal phenomena, then they should possess the following properties and characteristics:

1) The energy contained in one of the strongest corpuscular invasions must be adequate, at whatever level of efficiency its conversion into thermal energy takes place, effectively to trigger the change of the temperature of the entire polar stratosphere in a relatively short time and in the virtual absence of sunlight from normal midwinter to normal midsummer conditions, such as occurred in the massive stratospheric warmings of January 1963. Less intense solar events (corpuscular invasions) will be restricted in their significant thermal effects to above the 50 km level.

2) There must exist some fairly effective means of downward transmission in the upper atmosphere of the direct thermal and magnetostrophic wind effects of strong solar corpuscular penetration of the higher atmosphere to at least the 50 km level.

3) Strong solar corpuscular penetration of the upper atmosphere should be favored, either as to frequency of occurrence or lowest level of penetration in the atmosphere, or both, on the geomagnetic pole side of the hemisphere in the general region where the zone of maximum auroral frequency extends to its lowest geographical latitude.

4) The initial burst phase of a massive warming of the middle or upper stratosphere should be roughly comparable in areal extent to that of a major auroral display (strong solar corpuscular penetration of the upper atmosphere).

Basically, it is the first two of the required characteristics of solar corpuscular invasions as noted above that are essential to their operation as a **trigger** of sudden massive stratospheric warmings. They must bring a large part of the necessary energy with them, and this energy must be transmitted effectively downward from the level of its direct absorption in the higher atmosphere (~ 70-100 km) to the middle or lower stratosphere.

The forms of corpuscular radiation which merit attention for present purposes are:

1) Electrons, in the energy range 1-100 keV, which precipitate over the auroral zone, and also in the range up to 1000 keV;

2) protons, in the energy range 1-1000 MeV, originating in solar flares, and precipitating over the geomagnetic polar cap. Included in this latter group may be a proportion of α-particles, and possibly heavier elements.

Protons in the energy range 1-100 keV normally do not penetrate below 100 km, and hence are not considered as main phenomenon. All these phenomena tend to occur within the higher geomagnetic latitudes bounded by about magnetic latitude 45°, and mainly around $65\text{-}70^{\circ}$, but during major disturbances of the earth's magnetic field, extending a few degrees nearer the equator.

The depth or penetration of electrons into the atmosphere can be evaluated from known characteristics of energy loss, and by adoption of a model atmosphere. For example, a 10 keV electron may penetrate to a minimum altitude of 98 km, while a 400 keV electron will reach 64 km. There remains the question as the fraction of total energies which is available for heating the atmosphere. Chamberlain has estimated a fraction of about 15% as appearing as heat. Dalgarno estimates the fraction as about 20%, but does not exclude a value of 50%. The heat input from electrons in auroral latitudes and at altitudes of 90-120 km is thus of the order of 1 erg cm^{-2} sec^{-1} for solar maximum and for zonal and long term average flux. After major solar flares, the corresponding zonal average is probably at least one order of magnitude greater for periods of a few days.

In contrast to the zonal character of auroral electron precipitation, the incidence of solar protons is distributed over the polar caps. Incoming protons are assumed to move in Störmer trajectories, and the magnetic rigidity necessary to permit entry at a given angle to the vertical and at a given latitude may be calculated provided the spatial character of the earth's field is known. As a rough guide, the precipitation of solar

protons may be considered as bounded by the auroral zones, but in major events, marked effects occur as low as 50° geomagnetic latitude.

The lowest observed ionization from solar protons has been found at 42 km in the southern polar region during winter darkness. Loss of energy from an incident proton is continuous along the trajectory, but is essentially concentrated over the last few kilometers of path. Reid has calculated that a 50 MeV proton will lose 90% of its energy between altitudes of 50 and 42 km, 50% between 44.5 and 42 km, and 10% between 42.1 and 42.0 km. Hence, in a particular solar proton event, the increment of energy released in a given altitude range depends upon the spectrum of the flux and the geomagnetic latitude. An upper boundary of about 100 km is typical for most events, with release of energy down to a probable lower limit of 30 km in the largest events.

The main effects of particle precipitation are those which have been used extensively to determine the morphology of the precipitation zones, viz., optical excitation and electron-ion pair production. The effects of interest are the heating produced directly by the particle flux, and the possibilities of indirect effects. Among the latter may be included the modification of minor constitutuent concentrations, and the initiation of atmospheric wave motion. The conversion of the kinetic energy of incident particles into heat has been discussed by Bates and Chamberlain and the values of conversion efficiency used are between 0.15 and 0.5.

The major temperature increases are naturally associated with the largest fluxes of electrons in aurorae. Electrons in the energy range of 1-10 keV affect the altitude range 150-100 km, and here the increases in temperature during more intense fluxes occur at rates up to 100K min^{-1}. In general, due to the many factors which enter into a quantitative discussion of temperatures of the higher atmosphere, and also due to the difficulties of observation of this matter, the effects on the mesosphere of particle heating are not well known.

The possibility that particle influx might produce changes in concentrations of minor atmospheric constituents, and that the return to equilibrium of these concentrations might be on a longer time scale than the duration of intense fluxes, has been considered by a few workers. The dissociation of molecular oxygen by auroral electron and proton impact has been investigated by Maeda in relation to the warming of the polar mesosphere. He found that electrons, with a differential spectral distribution of the form E^{-4}, of a little over 10^{-8} cm^{-2} sec^{-1} at 80-85 km altitude. Protons, distributed according to a differential spectrum of $E^{-2.8}$, gave similar results, through the larger values than electrons below 80 km. This rate coefficient is nearly the same as that due to ultraviolet dissociation of O_2 in the Schumann-Runge continuum (1400-1750A), and the height of maximum dissociation is nearly the same, viz., 90 km. Thus, the process of dissociation by particles may be significant during large fluxes, especially in polar winter darkness.

The generation of traveling atmospheric waves is one consequence of particle precipitation, presumably due to a combination of spatial and temporal changes, including pulsations, in the incident flux, with corresponding changes in local heating. King refers to the evidence for these waves, which in some modes of propagation proceed from the auroral zones towards mid-latitudes with velocities ranging between 400 and 700 m sec^{-1}. Other workers have considered the heating aspect of these waves. Thus, these disturbances, though clearly associated with the auroral zone initially, may be included in the general subject of atmospheric wave motion, and the heating induced thereby.

APPENDIX C

Solar and Geophysical Indices

There is a wealth of operational data on solar and geophysical indices. The main problem is determining which data are pertinent for correlation analysis involving the upper atmosphere and the warmings. In view of the fact that no direct correlations have been found between stratwarmings and the upper atmosphere phenomena represented by the indices, the selection of the indices to be used must be made on the basis of a possible connection and not a probable one. In other words, we are dealing with a strictly exploratory situation inasmuch as no connection may exist between stratwarmings and higher atmosphere phenomena. Although meteorological research to date indicates that stratospheric warmings are caused by a transfer of energy from the troposphere to the stratosphere (Matsuno, 1971), nevertheless the possibility has not been completely ruled out that such events are triggered or enhanced by certain conditions occurring in the upper atmosphere above 80 km.

The solar and geophysical indices used are listed in Table 1; in-house values are indicated by a X mark for the months containing warmings. These particular indices were selected on a preliminary basis because they all appear to be correlated with upper-atmospheric heating phenomena. All of the indices except the HeII flux and D_{st} are available from the Environmental Data Service, NOAA, National Geophysical and Solar-Terrestrial Data Center, Boulder, Colo., in the monthly publication "Solar-Geophysical Data." Each index in Table I will now be discussed in turn.

TABLE 1

INDICES USED FOR STRATWARM ANALYSIS

INDEX	Apr '69	May '69	June '69	July '69	Aug '69	Dec '69	Jan '70	Dec '70	Jan '71	Jan '73	Feb '73
Solar Flares	X	X	X	X	X	X	X	X	X	X	X
Daily Flare Index						X	X	X	X	X	X
S.I.D.	X	X	X	X	X	X	X	X	X	X	X
Magnetic Condition	X	X	X	X	X	X	X	X	X	X	X
2800 MHz Solar Flux	X	X	X	X	X	X	X	X	X	X	X
HeII Solar Flux	X	X	X	X	X						
A_p	X	X	X	X	X	X	X	X	X	X	X
D_{st}	X	X	X	X	X	X	X	X	X		
AE	X	X	X	X	X	X	X	X			
Solar X-Rays (1-8A)	X	X	X	X	X	X	X	X	X	X	X
Solar Protons (>10Mev)	X	X	X	X	X	X	X	X	X		

Solar Flares

The power emitted by the sun is $\sim 4 \times 10^{33}$ ergs sec^{-1}, of which $\sim 5 \times 10^{24}$ ergs sec^{-1}, or 5 million horsepower per sq mile, irradiates the atmosphere of the earth. Ionizing x-rays and ultraviolet radiation, which constitute only $\sim 10^{-5}$ percent of the solar flux ($\sim 5 \times 10^{19}$ ergs sec^{-1}) are absorbed in the outer atmosphere to produce the ionosphere. A considerably greater amount of energy, $\sim 10^{20}$ ergs sec^{-1}, arrives at the magnetosphere in the form of solar-wind plasma, even under solar-quiet conditions. When the sun is intensely active, the energy delivered in ionizing radiations, both electromagnetic and corpuscular, can increase by orders of magnitude. No comparable energy supplies are available elsewhere in the sun-earth system.

A great flare on the sun can release $\sim 10^{32}$ ergs in x-ray ultraviolet and energetic-particle radiation. Every link in the system from sun to earth reacts to such a catastrophic event. After interacting with the interplanetary medium, the magnetosphere, and the upper atmosphere, the last residue of energy from the sun's explosive gift to earth is a faint red airglow that suffuses all the sky from north pole to south pole. Although the glow is composed only of the single, characteristic emission line of oxygen at 6300A, following a great flare the full sky may radiate 10^{23} ergs of this monochromatic energy.

A flare is a short-lived sudden increase in the intensity of radiation emitted in the neighborhood of sunspots. It is best seen in $H\alpha$, and usually occurs in the chromosphere. Flares are characterized by a

rise time of the order of minutes and a decay time of the order of tens of minutes. The total energy expended in a typical flare is about 10^{30} ergs; the magnetic field is extraordinarily high, reaching values of 10^{2} to 10^{4} gauss. Optical flares are usually accompanied by radio and x-ray bursts, or flares, and occasionally by high-energy particle emissions. The optical brightness and size of the flare are indicated by a two-character code called the importance. The first character, a number from 1 to 4, indicates the apparent area. For areas of less than 1, an "s" is used to designate a subflare. The second character indicates relative brightness; b for bright, n for normal, and f for faint. The most recent general discussion of solar flares is found in Smith and Smith (1963).

Hydrogen-α solar flare data are collected by numerous solar patrol stations over the globe. The February 1970 Solar-Geophysical Data Descriptive Text lists 53 stations. Data from these stations are found in the Solar-Geophysical Data bulletin and in the IAU Quarterly Bulletin on Solar Activity.

The Solar-Geophysical Data bulletin contains two listings of solar flare reports -- those published the month following the flare occurrence and those published 6 months after occurrence. The former list includes all reported flares of importance greater than one, giving the observatory, the date, the start time, the maximum and end times, the solar latitude and longitude, the McMath plage region, the duration in minutes, the importance, the observation condition and type, the area, and the maximum width of the Hα intensity. A 1-month listing of subflares is also provided indicating

date, time, and location. A full discussion of these parameters is found in the Solar-Geophysical Data Descriptive Text which appears in February of each year.

The listing published in Solar-Geophysical Data 6 months after occurrence consists of those flare reports filtered according to a program used at the Observatoire de Paris, 92 Meudon, France, to produce the IAU Quarterly Bulletin on Solar Activity flare listing. The format of the 6-month listing is the same as that of the 1-month flare listing described above. The grouped flare data appearing in the 6-month listing are also available from WDC-A, Boulder, on punched cards and magnetic tape for the period 1955 to the present.

As the number and refinement of observations increases, it becomes impressively clear that there is no single, simple flare model but rather a large spectrum of flare events which we can only crudely characterize by our conventional categories of class 1, 2, 3, faint, normal, and bright or by proton, hard x-ray, soft x-ray, white-light, and uv-continuum emissions or by "fast burst", "gradual rise," "fluctuating," and other phenomenological features. Many long-held and presumably firmly established concepts of ionospheric behavior have become open to question as a result of improved observational powers both in space and on the ground.

It used to be that ionospheric disturbance phenomena were studied as a means of estimating solar-flare x-ray and uv fluxes. But flare have now become diagnostic probes for ionospheric processes because the flare spectrum is directly measurable from space and the aeronomic cross sections for ion production processes are becoming known with considerable accuracy.

Daily Flare Index

The significant influence of solar flares on terrestrial disturbances of various kinds suggests that a daily flare index, similar to daily sunspot number or to the geomagnetic activity index, would be widely useful. Some studies may require construction of a special daily measure, tailored to fit the needs of the particular analysis, but a general expression of flare activity may suffice for a number of other studies.

The index published currently at the High Altitude Observatory corresponds closely to the index I_f to be described here. We shall call the present index "the new H.A.O. index," as most of our discussion pertains to the original definition. For an individual flare, the integrated intensity in Hα is defined as the product of four factors: relative brightness, apparent area, a factor depending on the fraction of area at maximum brightness, and duration. The sum of the integrated intensities of all the flares occurring on a given day is a quantitative estimate of the total excess solar energy due to flares. The clear physical interpretation of this index is augmented by other properties that are advantageous in many applications. Based on the apparent area and observed duration, this index gives a high weight to central flares. Its dependence on flare position is shared qualitatively by flare-associated radio and particle emission. The index also assigns a high weight to single large flares, as compared to numerous minor flares. This weighting also agrees with the probability of occurrence and the magnitude of sudden ionospheric disturbances. Thus, this index measures a definite physical quantity that is expected to bear a close relation to several interesting phenomena.

The daily flare index, calculated from the confirmed flares, is defined as

$$I_f = \frac{7600}{T^*} \Sigma A_d^2$$

where individual flare area A_d are measured in square degrees and T* is the effective observing time in minutes. Only those confirmed flares of greater than 1 square degree in area, as included in the IAU Quarterly Bulletin on Solar Activity, are used in calculating the flare index. I_f corresponds closely to the flare index developed at the High Altitude Observatory to measure the integrated intensity of flare radiation. The flare areas are not corrected for geometric foreshortening, so the definition of I_f places great weight on large flares, located near the center of the sun's disk. Characteristics of the index I_f are discussed in more detail in the paper by C. Sawyer "A Daily Index of Solar Flare Activity" (J. Geophys. Res. 72, 385, 1967).

The table lists the date, index and actual hours of observation included in the calculation and follows the table of confirmed Solar Flares.

Magnetic Condition

The magnetosphere is disturbed with varying frequency and intensity by perturbation in the solar wind. Changes in the solar wind dynamic pressure, whether sudden (as in discontinuities) or more gradual, result in a compression or expansion of the magnetosphere. The effects are transmitted inward as hydromagnetic waves and are manifested on the ground as an increase (for compression) or decrease (for expansion) in the magnetic field, representing a magnetospheric response of the simplest kind.

(1) Magnetospheric Substorms

Although the exact nature of the interaction between the solar wind and the magnetosphere at its boundary is not yet clear, there is increasing evidence that particles and other forms of energy are injected into the magnetosphere continuously or in bulk. It appears that when energy accumulated in the magnetosphere reaches a certain level, it is released rather abruptly in what is termed a magnetospheric substorm. The substorm involves a large-scale reorganization of the high-energy particle population, of the thermal plasma, and of the magnetic and electric fields in the magnetosphere; it also produces a severe magnetic disturbance on the surface of the earth at high latitudes, which is called a polar stat or magnetic substorm -- a complex phenomenon accompanied by other manifestations such as particle precipitation, auroral activity, infrasonic wave development, and generation of electromagnetic signals. Magnetospheric substorms often recur at intervals of 3 or 4 h, suggesting that this duration is the time constant for the buildup and release of energy in the magnetosphere.

As just mentioned, a magnetospheric substorm has a variety of manifestations over the entire earth, each of which may provide an important clue to the basic processes involved. Recent studies indicate that the magnetospheric substorm is associated with a sudden growth of electric fields. These electric fields generate the auroral electrojet in the polar ionosphere and accelerate auroral particles, which, in turn, can produce visible auroras and x-ray bursts when they interact with the atmosphere.

The study of polar magnetic substorms alone is not sufficient to understand the whole phenomenon of magnetospheric substorms. Intensive interdisciplinary studies of polar upper atmospheric disturbance phenomena are also needed. Compact, transportable, geophysical observatories equipped with identical standard instruments are suggested for such studies. A major effort in the analysis of polar upper-atmospheric disturbance phenomena should be directed toward the establishment of a model for the distribution of electric fields consistent with various manifestations of the magnetospheric substorm. The next step is to infer how these electric fields are produced as a consequence of the interactions between the "disturbed" solar wind and the magnetosphere. Such studies may provide clues to important problems, including: How can solar wind energy enter the magnetosphere? How is this energy stored and finally converted into the energy for a magnetospheric substorm?

(2) Geomagnetic Storms

The magnetosphere is severely disturbed during magnetic storms, which often occur about two days after an intense solar flare, or sometimes following the passage of a boundary in the interplanetary plasma sector structure. Several hours after the onset of a magnetic storm, a rapid succession of severe magnetospheric substorms occurs and the geomagnetic field is globally depressed owing to a formation of a ring current in the magnetosphere. Physical processes that take place during a magnetic storm are extremely complex and many are not well understood. The major processes involved and their effects as observed in the magnetic field at the ground are shown schematically in Figure 2 (National Academy of Sciences, 1969).

A typical geomagnetic storm has three phases: initial, main, and recovery (see Figure 3). A compression of the magnetosphere, manifested by a sudden commencement, is the major feature of the initial phase. The main phase is characterized by the growth of an intense ring current belt and frequently by severe magnetospheric substorms. During the development of the main phase, as many as ten magnetospheric substorms may occur in close succession, as illustrated in Figure 3 (National Academy of Sciences, 1969). These substorms are observed from the ground as a repetition of rapid growth followed by decay of the polar magnetic substorms. The "AE" index has been derived to express the activity of these polar magnetic substorms and thus of magnetospheric substorms.

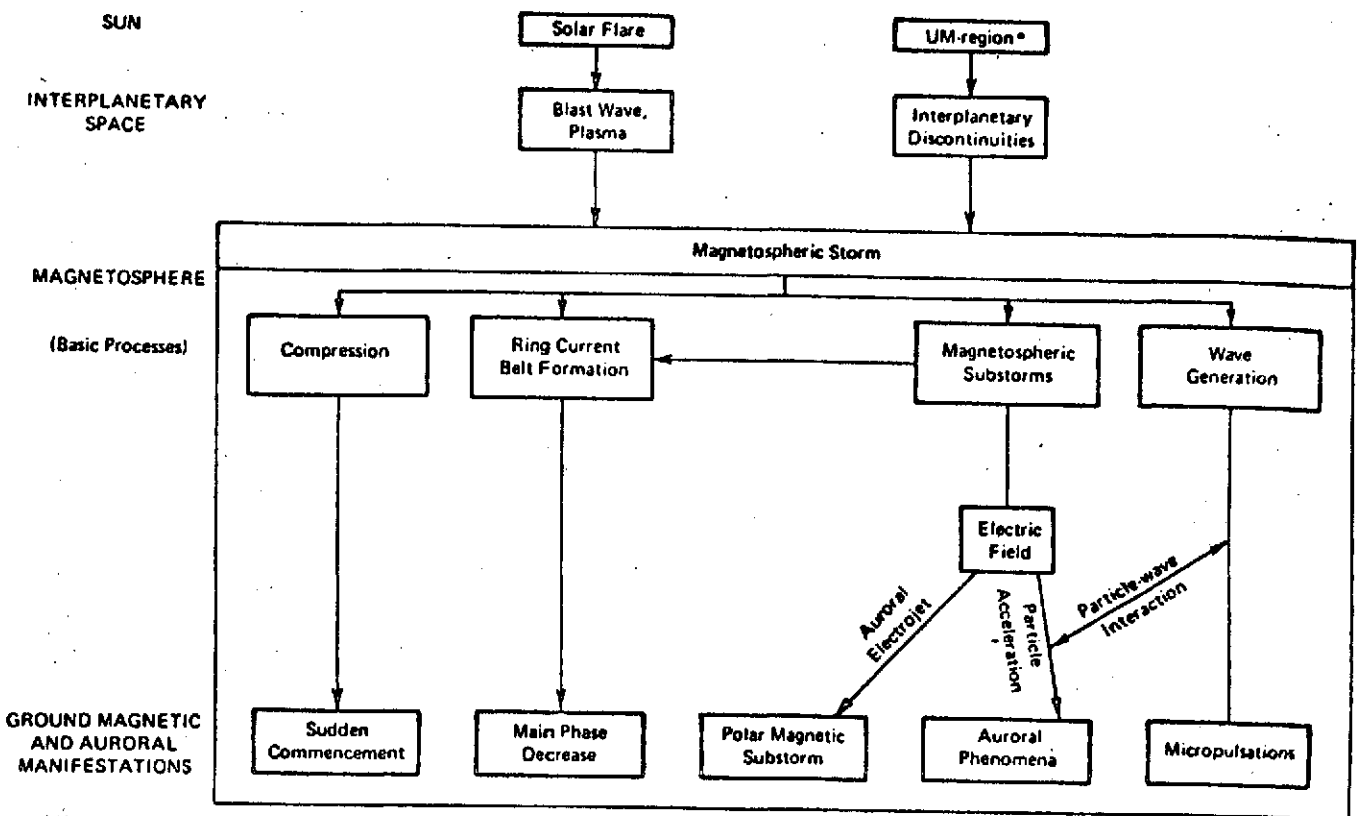

*UM-region, unipolar *M* region.

FIGURE 2 Schematic of major processes and their effects during a magnetic storm.

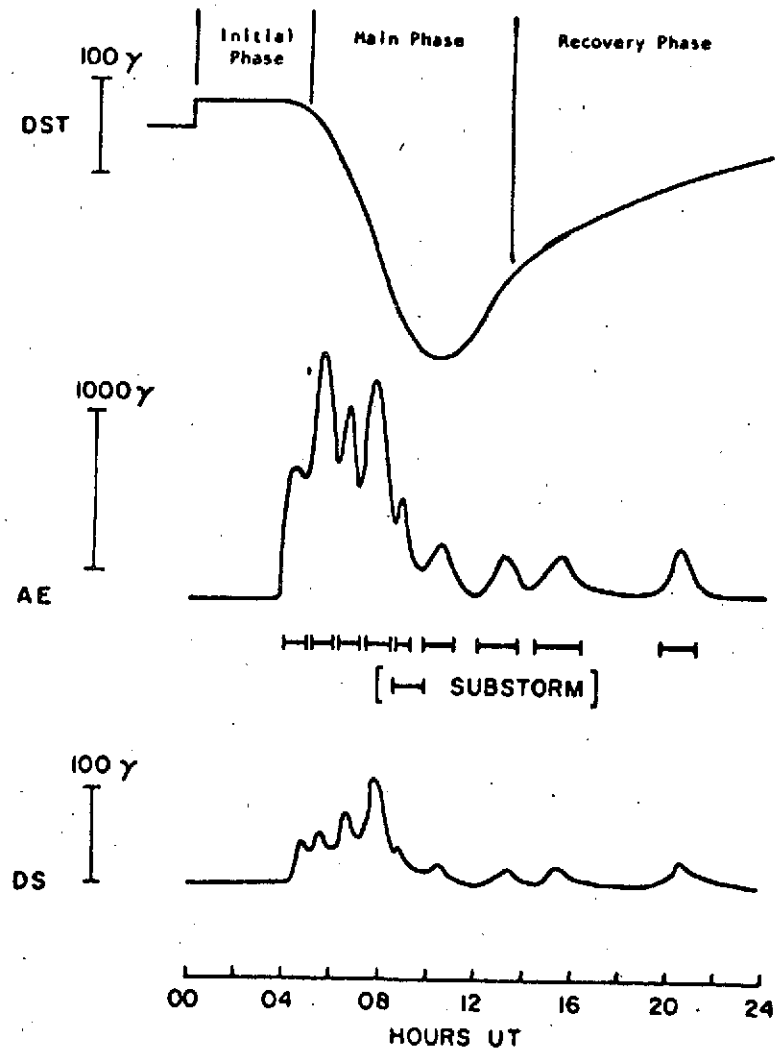

FIGURE 3 An example of a typical geomagnetic storm showing the three characteristic phases and the relationship between the Dst, AE, and DS indices. The Dst index is a measure of the magnetic field intensity of the ring current and also of the total kinetic energy of the ring current belt. The AE index is a measure of the intensity of magnetospheric substorms. The DS index is a measure of the magnitude of the asymmetry of the ring current field.

The ring current belt which develops during the main phase is predominantly composed of 5- to 50-kev protons. On the ground, the net effect of the ring-current system is a reduction of the horizontal component of the magnetic field in midlatitude and low latitude. An important aspect of the ring current belt is a large axial asymmetry during buildup. The "D_{st}" component represents the average intensity of the ring current field on the earth's surface, and "DS" gives the amplitude of the asymetric component. There is some indication that the time variation of DS is similar to that of the AE index, suggesting that the asymmetric component of the ring current is closely associated with magnetospheric substorms. An east-west chain of geomagnetic stations is vital for examining the instantaneous distribution of the asymmetric part of the ring current.

Typically, about 6 h after the onset of the main phase, the polar magnetic substorm activity begins to decay, while the main phase develops for an additional few hours. After the height of the main phase, the field begins to recover, sharply for a few hours and then more gradually with time. This can take several days or even longer.

In this report the indices D and S are used for magnetically-disturbed days and principal magnetic storms, respectively. The magnetically disturbed days (D) are selected in "Solar-Geophysical Data" in accordance with the general outline in Terrestrial Magnetism (48, 219, 1943). The method in current use calls for ranking the days of a month by their geomagnetic activity as determined from the following three criteria with

with equal weight: (1) the sum of the eight K_p's; (2) the sum of the squares of the eight K_p's; and (3) the greatest K_p.

A table in "Solar-Geophysical Data" presents the principal magnetic storms (S) for the month as reported by several observatories through cooperation with the International Association of Geomagnetism and Aeronomy.

Sudden Ionospheric Disturbances (SID)

Flares produce a variety of sudden ionospheric disturbances (SID), which can be resolved in height from the base of the D region to lower portions of the F region. Timing differences on a scale of a minute or less in the initiation of disturbances and in the rise to peak of the event can be highly diagnostic of the nature of the ionospheric production and loss processes when comparable data for ionizing fluxes are available directly from satellites.

Processes specific to the 60- to 75-km height range are:

1. Sudden phase anomalies (SPA), where the sky wave changes phase with respect to the ground wave as a result of an effective lowering of the reflection ceiling near the base of the D region, sometimes by as much as 16 km.

2. Sudden enhancement of atmospherics (SEA), manifested in improved reflection of very long radio waves (about 10,000 m) from the bottom of the D region. Distant tropical thunderstorms provide a steady background on a frequency of approximately 25 kHz, and signal strength may increase 100 percent during a large flare.

3. Sudden field-strength anomalies (SFA), observed as interference effects over medium distances between sky wave and ground wave when both are of nearly equal intensity. As the reflecting ceiling drops, the two waves vary in and out of phase, thus giving large variations in field strength at receiver.

In the 75- to 90-km range there occur sudden ionization increases which lead to:

4. Shortwave (5 to 20 MHz) radio fadeout (SWF), which is attributable to D region absorption. The phenomena is prompt to within a minute of flare outbreak.

5. Increased absorption of cosmic radio noise from outer space observed by riometers at approximately 19 MHz (SCNA).

To explore the ionosphere above 90 km we can observe sudden frequency deviations (SFD). An SFD is an abrupt increase in the frequency of a high frequency radio wave reflected from the F region followed by a slower decay to the transmitted frequency. The frequency deviation characteristically may exhibit several peaks near maximum and may even show negative deviations during the decay phase. In contrast with the D region effects that accompany 1- to 10-A x-rays, the SFD's are highly impulsive -- the rise to maximum is roughly a minute, and the source radiation is probably in the euv region from 10 to 1030A, most likely dominated by enhancement of the Lyman continuum radiation of hydrogen.

Observations of SFD in radio transmissions via the E and lower F regions have shown surprisingly fine temporal structure resolvable on a scale of only a few seconds. Without knowledge of the solar radiation flux, SFD's could serve as fast-resolving, broadband detectors of explosive flare outbursts. When combined with satellite flare measurements the SFD data can provide unique evidence of electron production rates and recombination coefficients. Recently it has become possible to record x-ray bursts with fine structure similar to SFD's, and it is remarkable that the SFD and

directly measured flux patterns are comparably sharp and can be matched to within 1 or 2 sec. From such comparisons it is possible to derive the concurrent solar euv continuum emission and to infer ionospheric reaction times far shorter than previously suspected.

SIDs are observed on the sunlit hemisphere and occur almost simultaneously with visual flare observations. SIDs and subsequent recovery of the ionosphere have a time duration somewhat longer than flare duration; generally from minutes to an hour, with rise more rapid than decay.

Several of the various SID observations are routinely identified and digitized. Samples of several types of original records as they appear before digitizing are nicely illustrated by Lincoln (1968). The types of SID are alphabetically listed below with brief descriptions of each. The SCNA, SEA, SES, SFD and SWF listings are available from the WDC-A for Upper Atmosphere Geophysics and have also been published in issues of Solar-Geophysical Data since 1963. Bursts and SFE are also listed in Solar-Geophysical Data. Information available in the data listings includes, in addition to that noted for PCA, the "definiteness" rated on a subjective scale.

Burst - A solar noise burst at riometer frequencies is a sudden increase of signal strength on the riometer records. This is caused by solar ratio noise emissions at riometer frequencies. This noise is affected by and can mask the ionospheric absorption that is present. The bursts are

of such short duration, however, that absorption changes during the burst can be estimated. In addition to riometer observations, solar noise is routinely observed at much higher frequencies than those used for riometer receivers.

Crochet - see SFE.

SCNA - Sudden Cosmic Noise Absorption, also referred to as CNA (Cosmic Noise Absorption) Type I (see below), is characterized on riometer recordings by a sudden daytime absorption increase of several db within a few minutes. Decay is somewhat slower than rise, and the riometer record is perturbed for a period of minutes to over an hour. SCNA involves absorption outside of auroral regions.

SEA - Sudden Enhancement of Atmospherics is observed asan increase in signal strength on wideband equipment operated to detect electromagnetic emissions from lightening. This equipment operates in the VLF (10 to 50 kHz) range with the most commonly used frequency near 27 kHz.

SES - Sudden Enhancement of Signal is observed on VLF frequencies (15 to 50 kHz). These observations are nearly identical to SEA except that the receivers are narrow-band receivers designed to pick up man-made VLF transmissions. As with SEA, signal strength increases is the SID indicator.

SFD - Sudden Frequency Deviation, caused by ionospheric disturbances, is observed by beating the received radio signal with a reference frequency that is near the received frequency. This technique allows small frequency changes to be observed. SFD is observed in the high-frequency range,

and the reference signal is obtained locally from a stable oscillator. Occurrence times and deviations in frequency are listed in data presentations.

SFE - Solar Flare Effect, or crochet, is observed as a small hook on magnetometer records. It is caused by the magnetic field response to increased current flow in the E region due to electron enhancement induced by flare x-rays.

SPA - Sudden Phase Anomaly is observed in the same manner as SFD, except that VLF frequencies are used and the reference signal is the ground wave. For observing SPA on transmitters more distant than possible for ground wave propagation (about 200 km), the ground wave reference signal is provided by telephone or a local reference signal source is used as in SFD observations.

SWF - Short Wave Fadeout is observed from signal strength records of any shortwave (3 to 30 MHz) receiver. Signals from sweep-frequency ionosondes (vertical or oblique incidence) may be completely absorbed. SWF is categorized as gradual (G), slow (Sl), or sudden (S), depending primarily on how rapidly the signal loss occurs.

CNA

In addition to SCNA discussed under SID, there are two other types of CNA. Data on these latter types are not generally available but are mentioned here to broaden perspective. Cosmic Noise Absorption is observed

on riometers that operate between 15 and 60 MHz, but most often near 25 MHz. Absorption is normalized to low nighttime absorption occurrences for that station. CNA can be divided into SCA (sudden commencement absorption), CNA Type I, also called SCNA (sudden cosmic noise absorption), and CNA Type II. CNA Type II is local nighttime absorption associated with active aurora. The absorption may persist for hours with irregular variation including individual peaks as high as 8 to 10 db persisting for several minutes. This is sometimes called auroral absorption, but is not the same as AZA, which is not a local phenomenon.

SCA (Sudden Commencement Absorption) is characterized by sudden onset, occurrence in zones centered on the auroral zone (58° to 75° geomagnetic), and persistence for less than 1 hour. The SCA is similar to SCNA in rise time and duration. Type I and II CNA are somewhat local and irregularly distributed in longitude in contrast to the zonal occurrence of SCA. SCAs have been associated with geomagnetic storm sudden commencement x-ray fluxes.

2800 MHz (10.7 cm) Solar Flux

Within the past 20 years, radio observations have provided a new means of probing the temperature and electron distributions in the solar atmosphere with the resultant possibility of providing other indices of solar activity. In particular, it has been found that the intensity of radio emission fromthe whole disk above a certain minimum value varies from day to day and in the vicinity of 3000 MHz the variations correlate well with the Zurich relative sunspot numbsers or the total area of sunspots present on the disk. Sudden enhancements in the emission or bursts occur and can be separated readily from the background daily level to provide a second radio indication of solar activity closely associated with flare appearances. It has been found that the intensity of the daily level and of the bursts changes slowly with frequency in the band from 1000 to 9000 MHz so that any observations made on a single frequency in the center of this band can be regarded as typical and provides most of the information. The routine observations of the sun at a wavelength of 10.7 cm (2800 MHz) were commenced in 1947 at Ottawa by the Radio and Electrical Engineering Division of the National Research Council and have provided observations suitable for establishing a radio index. It has been found that the single value obtained at local noon is sufficient for most applications.

The correlation between the orbital deceleration of an artificial satellite and the solar radio flux in the decimeter range has led to relationships between the atmospheric density at various heights and the 10.7- and 20-cm radio fluxes. Considering that the density variation is due to a temperature variation, it can be concluded that the solar extreme ultraviolet

radiation (EUV) is responsible for the heating of the upper atmosphere and that heat conduction is responsible for its cooling. A change in the ultraviolet radiation can be correlated with a change in the radio flux just as with the sunspot number, which is a well-known index of solar activity. The 10.7-cm and EUV should be correlated in some degree, inasmuch as many features of the sun vary with the solar cycle, including the number of sunspots, faculae, filaments, prominences, flares, and height of the chromosphere and shape of the corona. With regard to the radio waves represented and optical manifestations in the EUV regions, however, no exact casual relation between these groups of phenomena has been advanced. Although it is true that both radiations issue from the upper chromosphere and lower corona, our knowledge of the details of their origin is very deficient. At present, there are no theoretical grounds for an exact relation (Anderson, 1965).

Daily observations of the 2800 MHz radio emissions which originate from the solar disk and from any active regions are made at the Algonquin Radio Observatory (ARO) of the National Research Council of Canada with a reflector 1.8 meters diameter. These are a continuation of observations which commenced in Ottawa in 1947. Numerical values of flux in the tables refer to a single calibration made near local noon at 1700 UT. When the flux changes rapidly, or there is a burst in progress at that time, the reported value is the best estimate of the undisturbed level and provides the reference level for measuring the burst intensity. The various types of outstanding events are listed separately in another table. The observed

flux values have variations resulting from the eccentric orbit of the earth in its annual path around the sun. Although these radio values are suitable to use with observed ionospheric and other data, an adjustment must be introduced when the observations are used in studies of the absolute or intrinsic variation of the solar radio flux. Thus, the tables show both the observed flux, S, and the flux adjusted to 1 A.U., S_a. The observations are made for a single North-South polarization but reduced for the assumption of two equal orthogonal polarizations. A graph showing the monthly highs and lows for the last two sunspot cycles is shown in Fig. 4. Relative errors over long periods of time are believed to be $\pm$ 2 percent, over a few days may be $\pm$ 0.5 percent. The characteristics of the observations are surveyed in "Solar Radio Emission at 10.7 cm" by A.E. Covington [J. Royal Astron. Soc., Canada, 63, 125, 1969]. Experiments conducted during the past few years indicate that a multiplying factor of 0.906 should be applied to the reported flux values in order to derive the absolute flux value.

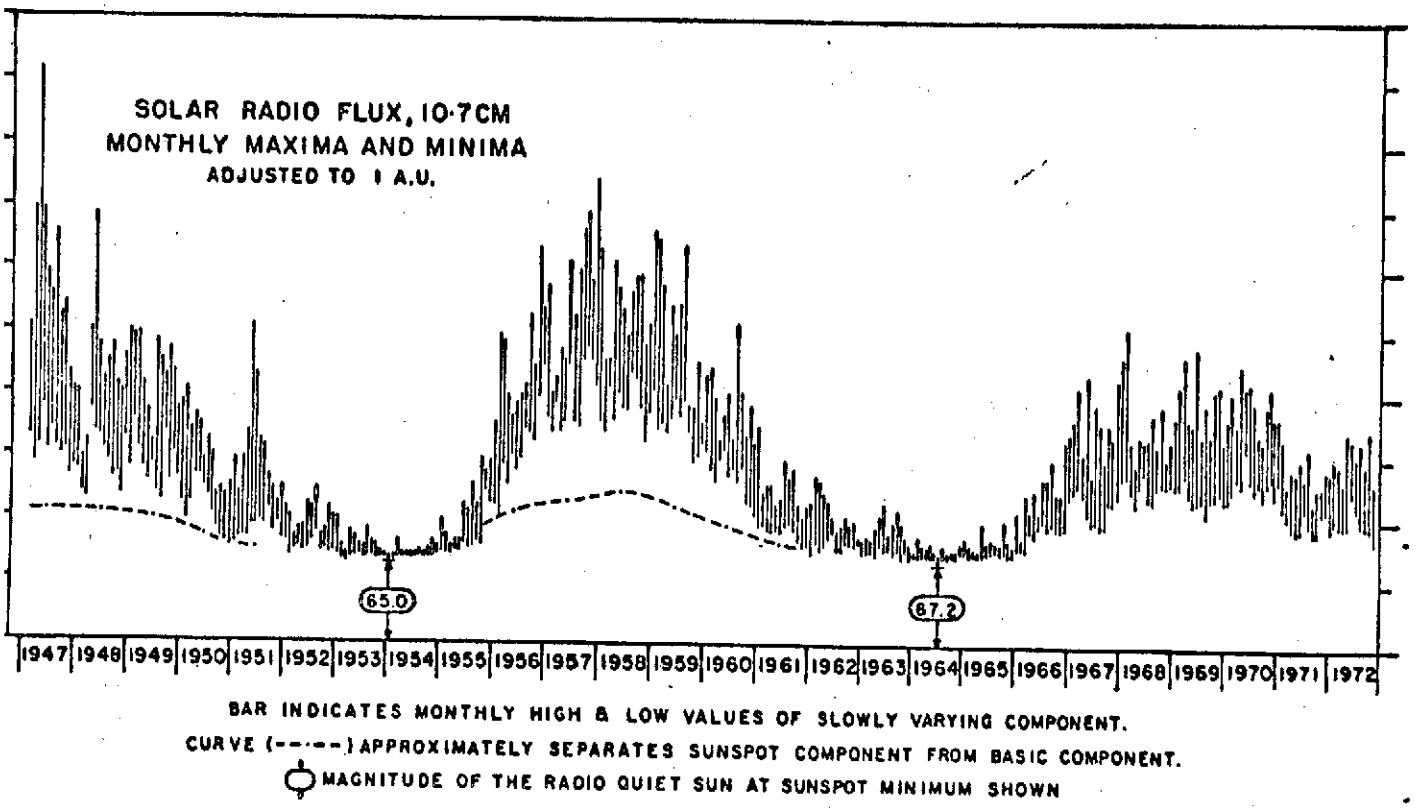

.g. 4 Monthly Maxima and Minima of 2800 MHz (10.7 cm) Solar Flux, 1947-1972.

HeII Solar Flux

Many workers have carried out the detailed calculations to determine how much of the incident solar UV energy is converted to heat in the thermosphere near 140 km, and how much dissociates and excites oxygen and nitrogen molecules. The mean free path in the thermosphere is so large that only a small amount of recombination and de-excitation occurs there. In order for these processes to occur, the atoms and excited molecules must diffuse down into the mesosphere. It is there that this energy is ultimately recovered and converted to heat. According to the latest estimates, about 70 percent of the solar UV energy is converted to chemical energy.

Most of the chemical energy is converted to heat in the altitude range 70 to 90 km, through two recombination processes: One process involves the production of O_2 and O_3. The other process involves de-excitation.

The extreme ultraviolet line of HeII at 304A contains much of the energy involved in heating the atmosphere near 140 km. The measurements at 304A were obtained from Timothy and Timothy (1970) for April-August 1969. These data are a more accurate index than the 2800 MHz solar flux of the upper atmospheric EUV heating (Anderson, 1965).

Solar Protons (Greater than 10 Mev)

Significant numbers of charged particles, mainly electrons and protons, are accelerated at the sun during many solar flares. Some of these particles are subsequently detected within the interplanetary medium and at the earth. These particles serve as useful indicators of solar, terrestrial, and interplanetary conditions. Often, effects from these various regions are not separable, but in certain events they are.

A series of Solar Proton Monitoring Experiments (SPME), initiated by scientists at Johns Hopkins University /Applied Physics Laboratory and at NASA Goddard Space Flight Center, is intended to provide reliable flux and spectral measurements of solar protons over at least half a solar cycle and over a wide flux range. Each SPME consists of an array of solid-state detectors that measure the combined counting rate due to fluxes of protons and alpha particles in each of the three energy ranges: ≥10 Mev/nucleon, ≥ 30 Mev/nucleon, and ≥ 60 Mev/nucleon. The alpha particle component is usually very small and may be thought of as introducing an ambiguity of less than 10 percent into the proton count rate. Further discussions of this point and of the SPME in general can be found in the "Descriptive Text" of Solar-Geophysical Data (February 1970).

The SPME was successfully launched aboard the NASA satellites Explorers 34 (IMP-F, 1967-51A) and 41 (IMP-G, 1969-53A) on May 24, 1967 and June 21, 1969, respectively. Explorer 34 re-entered the earth's atmosphere on May 3, 1969 and Explorer 41 re-entered on December 23, 1972. Continuous data

from the SPME have been presented for the lifetimes of Explorers 34 and 41. Similar equipment was launched aboard Explorer 43 (IMP-I, 1971-19A) on March 13, 1971 and these data have been used to supplement the Explorer 41 data, and will continue in 1973.

The primary purpose of the SPME is to provide systematic monitoring of solar cosmic rays over at least half a solar cycle. The basic requirements set forth for such a monitoring program were:

1) to furnish simple reliable flux and spectral measurements,
2) to operate over a wide flux range and in particular provide coverage for very large events,
3) to provide a simple and easily reproducible detector system to form the basis of an operational monitoring program.

All data fromthe SPME published as monitoring data satisfy the following requirements:

1) final orbit determinations have been made,
2) final time corrections have been made,
3) all data quality flags indicate that the individual data point is "good."

Data that satisfy these requirements are then used to construct hourly averages of the respective energy channels. The ≥60 Mev and ≥30 Mev channels are sampled for 19.2 seconds once every 2 minutes 43.8 seconds, The ≥10 Mev channel is sampled twice every 2 minutes 43.8 seconds at 19.2 seconds per sample. Thus, the maximum number of points in an hourly average

is 22 for the ≥ 60 Mev and ≥ 30 Mev channels and 44 for the ≥ 10 Mev channel. If the number "good" data points is less than 5, the hourly average is not constructed.

These hourly averages are then tabulated in a grid where the hours of the day run to the right and the days of the month run from top to bottom. The day is identified as both day of the month and day of the year. The tabular entries are nominally four characters each. The decimal point will be automatically shifted to the right as the intensity increases until it finally disappears when the intensity is ≥1000 protons $cm^{-2}sec^{-1}$. If the intensity becomes ≥ 10,000 protons $cm^{-2}sec^{-1}$, the blank space between columns is utilized so that intensities up to 99,999 protons $cm^{-2}sec^{-1}$ may be accommodated. The entries all begin with a low intensity format of 0.XX. The following is an example of how the entries appear for an intensity increasing from 0.55 protons $cm^{-2}sec^{-1}$ to 55,000 protons $cm^{-2}sec^{-1}$.

0.55
5.50
55.0
550.
5500
55000

The hourly averages are also plotted vs. time in monthly blocks. The response of the ≥ 10 Mev channel in the radiation belts is very noticeable since this channel also responds to electrons of energy ≥ 515 kev. This low an electron energy threshold makes this channel respond to the radiation belt

for a much larger radial extent (at times out to 10 earth radii) than channels 1 and 2 whose electron thresholds are several Mev in energy. The actual time profiles, due to the radiation belts, displayed by the ≥10 Mev channel on the hourly plots are highly variable due to the great variations in these trajectories through the trapping regions.

The Magnetic Index A_p

Types of solar-terrestrial correlations and more recent space observations demonstrate, when viewed in total, that magnetic activity on the earth is very closely related to solar phenomena. This has already been discussed to some extent in the section "Magnetic Condition."

To facilitate correlations with other phenomena, both terrestrial and solar, and to have simple criteria for relating changes in magnetic activity from hour to hour, day to day, month to month, etc., various indices of magnetic activity have been proposed and used. Two of the oldest are: C, the daily character figure on a scale of 0 to 2, which is a simple numerical, but qualitative, estimate of the day's activity at each observatory, and U which is a measure of the change in the average value of the horizontal component from day to day.

In the past two decades considerably more use has been made of an index called K, when given for a single observatory, and K_p, when given for a select group of observatories which we will describe below. K_p, in particular, has been used extensively in space studies both for characterizing solar-terrestrial conditions and for correlating in detail magnetic activity with numerous types of space measurements ranging from magnetospheric neutral particle densities to cosmic rays. Thus, it is important that we have some understanding of the meaning of K_p.

The K-index of a station is a quasi-logarithmic measure of the local magnetic activity obtained in 3-hrly. intervals of the Greenwich day. It

is related to the maximum range in the 3-hr. interval of the most disturbed component of the magnetic field. The index assumes values between 0 and 9 corresponding to the quietest and most disturbed conditions, respectively. Since the degree of magnetic activity as measured by the range in gammas is strongly latitude-dependent, the different magnetic observatories must apply appropriate scaling factors to convert the gamma-range to K-index in order that the frequency distribution of K-indices be the same for all observing stations. Thus, a K of 9 would represent a range of at least 300 gammas at low latitudes and 2500 gammas in the auroral zone. More than 80 stations currently provide K-indices.

The planetary index K_p is the average of 3-hourly K-indices from 12 selected observatories located in middle geomagnetic latitudes from 47° to 63°. All but one of the stations are located in the northern hemisphere. The index is commonly used as a measure of the global average magnetic activity. However, it must be borne in mind that conditions in polar and equatorial regions may not conform with the planetary K_p.

A linear scale of disturbance values a_p has been adopted corresponding to the quasi-logarithmic values K_p. Each Greenwich day has 8 a_p-values corresponding to the 8 K_p-values. The daily average of a_p is called the daily planetary amplitude and is denoted A_p. High values of this index are definitely associated with upper atmosphere heating although the heating mechanism is not completely understood (Anderson, 1973).

The 3-hourly K_p and daily A_p values for each month are published (with a 2-month lag) in the Solar-Geophysical Data (Prompt Reports), Part I, CRPL-FB 135^{+}, U.S. Dept. of Commerce, Boulder, Colo., USA 80302.

The AE Index

Although the A_p index is capable of describing the general state of planetary geomagnetic activity, it contains contributions from at least two major sources, the auroral electrojet and the ring current. To study auroral-zone activity it is desirable to maximize the auroral electrojet contribution. This has been accomplished by the development of the AE index. To obtain this index of geomagnetic activity, only slightly sub-auroral-zone stations are employed for the most part, and they are chosen so as to provide uniformly spaced coverage around the auroral zone. In some cases this necessitates the use of southern hemisphere stations to take advantage of the apparent conjugacy of magnetic variations of a substorm nature.

The AE index is constructed by using only the H component of the perturbation field. The H component at each observatory is scaled at 2.5-min intervals; the average quiet-time baseline is used as a reference level. These baseline levels are assumed to be within $\sim$ 10 gamma of the undisturbed H component, and thus the actual scaled values of ΔH include S_q contributions in addition to those from the auroral current system.

All the scaled values from the various observatories are superimposed in a magnetogram format. This composite drawing is enclosed by upper and lower envelopes representing the maximum positive and negative values of ΔH for all observatories at each given time. The amplitude of the upper envelope at any instant is denoted by AU, and the amplitude of the lower envelope is designated by AL. If the station distribution were

closely enough knit, AU and AL would represent the maximum positive and negative deviations occurring along the auroral zone.

Physically speaking, AU gives a good representation of the maximum magnetic perturbation generated by the eastward electrojet usually found in the afternoon sector. Similarly, AL represents the maximum magnetic perturbation generated by the westward electrojet in the morning and midnight sectors. At the present time it appears as though the eastward and westward electrojets may fluctuate independently of one another, so that it may be useful to treat AU and AL as independent indices. However, at the present time it is customary to combine these indices to give a direct measure of the total maximum amplitude of the eastward and westward electrojet currents. Hence, the index AE is defined by AE = AU - AL. Thus, AE represents the difference in levels (measured in gammas) between the upper and lower envelopes at any given instant in time.

Although AE is generally calculated at 2.5-min intervals and is available in this form from the World Data Center, hourly average values of AE are also available for the period 1957-1964, inclusive (University of Alaska Reports UAGR-192, UAGR-200). More recent AE index values through 1970 are available from the National Space Science Data Center, Goddard Space Flight Center, Greenbelt, Md. 20771.

Observations of traveling ionospheric disturbances emanating from polar regions has led to the suggestion that auroral energy may be coupled to atmospheric wave motions through heating produced by ohmic dissipation

of electric currents, joule heating. Cole's (1962) pioneer work has established that joule heating in the region 100-200 km could lead to large temperature changes, through heat flux by thermal conduction in the vicinity of 150 km and above. However, below 150 km it appears that the relaxation time, i.e., the time it takes an initial temperature impulse T_i to fall to $e^{-1}T_i$, is at least one day and is independent of T_i. On this basis, short period gravity waves ($\sim$ 1 hr) should transfer energy more efficiently than conduction below about 150 km, if the vertical scale of the propagating waves is approximately greater than the local scale height and if the coupling of auroral heating into gravity wave energy is efficient. Blumen and Hendl (1969) have investigated Joule heating in the vicinity of the auroral electrojet (100-150 km).

The D_{st} Index

The D_{st} index provides a planetary magnetic index on a hourly basis that has been used extensively in studies of geophysical disturbances, particles and plasma in the magnetosphere, solar-terrestrial relationships, and cosmic rays (Suguira and Cain, 1969).

Equatorial D_{st} is a measure of the mean departure from normal of the horizontal component, H, of the Earth's magnetic field observed at a group of low-latitude stations, whereas a_p is based on 3 hr ranges of the field at stations in higher latitudes.

The strength of D_{st} lies in its ability to detect all magnetic storms. This stems from the fact that the ring current is world wide in nature, and thus there is little or no possibility of D_{st} not reacting to the growth of the ring current. Furthermore, within about two hours, the D_{st} index should be able to identify the onset and termination of the main phase of a magnetic storm (during which time the major portion of the energy of the storm is dissipated in the magnetosphere). Thus, the D_{st} index gives a good qualitative description of the gross level of magnetospheric activity at any time, although it cannot be used to reveal the presence of individual substorms.

The values of D_{st} used in this analysis came from Goddard Space Flight Center reports (see for example, Sugiura and Poros, 1971).

Solar X-Rays (1-8A)

This index is used to indicate the magnitude of the x-ray flux between 1-8A which can cause atmospheric heating between 55-105 km. Solar x-ray emissions, like solar radio emissions, originate from both thermal and nonthermal processes that take place primarily in the solar corona. Solar x-ray emissions can be divided into three components: the quiet sun component, the slowly varying component, and the burst component. Nonthermal x-ray emissions occur only in the hard x-ray emissions (photon energies greater than about 10 kev or wavelengths less than about 1A) accompanying solar flares. Solar x-ray astronomy has been reviewed by Krimigis and Wende (1970).

Solar x-rays are directly observed with satellite-born detectors and indirectly observed through their effects on the ionosphere. The occurrences of solar x-ray bursts are indicated by the sudden ionospheric disturbances (SID). Patrol types of solar x-ray measurements must be carried out using instruments flown on satellites. Because solar x-ray instrumentation must be flown on satellites, the data quite often contain periodic and signifiant time intervals when no data were obtained due to the satellite's being eclipsed.

Ion chambers, proportional counters, Geiger tubes, and scintillators are used to measure the integral solar x-ray flux within specific wavelength or energy passbands. A review of such instrumentation is given by Neupert (1969).

Solar x-ray fluxes, integrated over the entire solar disk in units of ergs $cm^{-2}sec^{-1}$ over a specified passband, have been obtained from several satellites. The x-ray fluxes are useful and sensitive indicators of the level of solar activity.

The data used in this report consist of tables of hourly averages of x-ray flux in the 1 to 8A band. The primary source of the data is the Naval Research Laboratory's SOLRAD 9 and 10 satellites. Each satellite stores 0.5 to 3A, 1 to 8A, and 8 to 20A data in the satellite memory with a one minute time resolution. Therefore, a continuous record of the x-ray emission from the sun, except for gaps due to satellite night and charged particle interference, is available for these three bands. A complete description of the SOLRAD 10 experiments is given in NRL Report No. 7408 titled "The SOLRAD 10 Satellite, Explorer 44, 1971-058A." A complete description of the SOLRAD 9 experiments is given in NRL Report No. 6800 titled "The NRL SOLRAD 9 Satellite, Solar Explorer B, 1968-17A."

The data from the 1 to 8A ionization chamber are converted to a 1 to 8A energy flux based on a 2×10^6K gray-body solar emission spectrum (Kreplin, R.W., Annales de Geophysique, 17, 151, 1961). The averages include data obtained during solar flares but data contaminated by charged particle interference are excluded wherever possible. When SOLRAD 10 data for an hour are missing, SOLRAD 9 data are used. Measurements by the SOLRAD 9 and SOLRAD 10 1 to 8A ionization chambers are virtually identical so normalization is not required. For identification purposes only, the SOLRAD 9 data are followed by the symbol <. The values given for each

hourly average are in units of 10^{-3} ergs/cm^2 sec, and the time scale is UT. The tabular entries are made with a shifting decimal point. Therefore, the values which may be expressed in the four spaces assigned to each entry range from .001 to 9999 times the basic unit, 10^{-3} ergs/cm^2 sec.

APPENDIX D REFERENCES CITED IN APPENDICES A-C

Anderson, A.D; "The correlation between low-altitude neutral density variations near 400km and magnetic activity indices,"Planet Sp.Sci. 21, 2049, 1973.

Anderson, A.D.; "Long-term (solar cycle) variation of the extreme ultraviolet radiation and 10.7-centimeter flux from the sun," J. Geophys. Res. 70, 3231, 1965.

Blumen, W. and R.G. Hendl; "On the role of Joule heating as a source of gravity-wave energy above 100 km," J. Atmos. Sci. 26, 210, 1969.

Clark, J.; Monthly Wea. Rev. 98, 443, 1970.

Cole, K.D.; "Joule heating of the upper atmosphere," Australian J. Phys. 15, 223, 1962.

Groves, G.V.; "Seasonal and latitudinal models of atmospheric temperature, pressure, and density, 25 to 110 km," AFCRL-70-0261, 1970.

Hirota, I.; "The vertical structure of the stratospheric sudden warming," J. Meteor. Soc. Japan 45, 422, 1967.

Houghton, J.T. and S.D. Smith; "Remote sounding of atmospheric temperature from satellites," Proc. R. Soc. London A 320, 23, 1970.

Krimigis, S.M. and C.D. Wende; Solar Eclipses and the Ionosphere, ed. M. Anastassiades, Plenum Press, New York, 1970.

Labitzke, K.; "Synoptic-scale motions above the stratosphere," NCAR 71-139, 1971.

Lincoln, J.V., Reporting of sudden ionospheric disturbances, Ann.IQSY, 1, 196[illegible].

Matsuno, T.; "A dynamical model of the stratospheric sudden warming," J. Atmos. Sci. 28, 1479, 1971.

Muench, H.S.; "Stratospheric energy processes and associated atmospheric long-wave structure in winter," AFCRL Environmental Res. Paper 95, 1965.

References (Cont'd)

National Academy of Sciences, Physics of the Earth in Space, National Research Council, Washington D.C., 1969.

Neupert, W.M.; "X-rays from the sun," Ann. Rev. of Astron. and Astrophys. 7, 121, 1969.

Rodgers, C.D.; "Remote sounding of the atmospheric temperature profile in the presence of cloud," Quart. J. Roy. Met. Soc. 96, 654, 1970.

Smith, H.J. and P. Smith; Solar Flares, Macmillan Co., New York, 1963.

Sugiura, M. and S.J. Cain, NASA Goddard Space Flight Center Rep. X-612-69-20, 1969.

Sugiura, M. and D. Poros; "Hourly values of equatorial D_{st} for years 1957 to 1970," Goddard Space Flight Center Rep. X-645-71-278, 1971.

Timothy, A.F. and J.G. Timothy; "Long-term intensity variations in the solar Helium II Lyman Alpha Line," J. Geophys. Res. 75, 6950, 1970.

Trenberth, K.E.; "Dynamical coupling of the stratosphere with the troposphere and sudden warmings," MIT, Dept. Meteorology, Ph.D. Thesis, Jan. 1972.

Webb, W.L.; Structure of the Stratosphere and Mesosphere, Academic Press, New York, 1966.

APPENDIX E

ADDITIONAL REFERENCES - STRATOSPHERIC WARMINGS

Aanensen, C. J. M; "The Use of Nimbus 4 Radiance and Radio-Sonde Data in The Construction of Stratospheric Contour Charts," Quart. J. Royal Met Soc., Vol. 99, pp 657-668, 1973

Chiu, Y. T; "Thermospheric Convective Instability," Space Research XII, pp 1025-1028, 1972.

De Vries, L. L.; "Structure and Motion of The Thermosphere Shown by Density Data from The Low-G Accelerometer Calibration System (LOGACS)," Space Research XII pp. 867-879, 1972

Faire, A. C. and Murphy, E. A; "Perturbations in Density and Temperature Height Profiles Obtained at Elgin, Florida," Space Research XI, pp 821-828, 1971

Gaigerov, S. S., M. YA. Kalikhman, V. E. Sedov, E. G. Shvidkovsky, D. A. Tarasenko, and B. P. Zaichikov; "Vertical Distribution of the Main Meteorological Parameters and Large-Scale Processes in the Stratosphere and Mesosphere," Space Research XI, pp. 799-805, 1971

Hook, J. L.; "Wind Patterns at Meteor Altitudes (75-105 Kilometers) Above College, Alaska, Associated with Midwinter Stratospheric Warmings," J. Geophysical Res., Vol. 77, No. 21, July 20, 1972, pp. 3856-3868.

Kokin, G. A., Yu. N. Moiseev, V. F. Tulinov and I. G. Shapiro; "Corpuscular Fluxes and Mesopheric Temperatures During Periods of Elevated Solar Activity," Space Research XI pp. 923-928, 1971

Koshelkov, Yu. P.: "Synoptic Processes and Structure of the Upper Atmosphere in the Southern Hemisphere," Space Research XI, 1971, pp. 793-798

Labitzke, K., and H. Van Loon; "The Stratosphere in the Southern Hemisphere," Chapter 7 of Meteorological Monographs, Vol. 13, No. 35, 1972, pp 113-138, American Meteor. Soc.

Leovy, C. B. and T. Ackerman; "Evidence for High-Frequency Synoptic Disturbances Near the Stratopause," J. Atm. Sci., Vol. 30, No. 7, July 1973, pp 940-942

Olson, W. P.; "Corpuscular Radiation as an Upper Atmospheric Energy Source," Space Research XII, 1972, pp. 1007-1013

Quiroz, R. S., M. P. Weinreb, D. Q. Wark; "Operational Radiance Maps of the Stratosphere, with Preliminary Details of a Major Stratospheric Warming," presented at the 16th COSPAR meeting, May 23-June 6, 1973, Konstanz, Germany.